Catalysis Letters 62 (1999) 159–167

Selective production of hydrogen by partial oxidation of methanol over catalysts derived from CuZnAl-layered double hydroxides

S. Velu, K. Suzuki * and T. Osaki

Ceramics Technology Department, National Industrial Research Institute of Nagoya, 1-1 Hirate-cho, Kita-ku, Nagoya 462-8510, Japan
E-mail: ksuzuki3@nirin.go.jp

Received 26 June 1999; accepted 27 August 1999

Hydrogen production by partial oxidation of methanol (POM) reaction ($CH_3OH + (1/2)O_2 \rightleftharpoons 2H_2 + CO_2$) was investigated over a series of CuZnAl ternary oxide catalysts derived from CuZnAl hydroxycarbonate precursors containing hydrotalcite-like layered double hydroxide as a major phase. These catalysts exhibited a good catalytic activity and high H_2 selectivity. A methanol conversion of about 40–60% was obtained at 200 °C with high selectivity of H_2 and CO_2. The undesirable by-product, CO was virtually not produced over most of the catalysts at this temperature. The catalytic activity was found to decrease with increasing (Cu + Zn)/Al atomic ratio in the precursor and, was correlated with Cu metal surface areas, Cu dispersion and Cu particle sizes, which were calculated by both XRD and TPR-N_2O passivation methods. The catalyst with higher Cu surface areas and Cu dispersion displayed a higher catalytic activity. Lifetime experiments showed that these catalysts were stable over a period of 24 h of continuous operation. Catalyst precursors containing hydroxycarbonates other than LDH as a major phase offered considerable amount of dimethyl ether as a by-product.

Keywords: hydrogen production, methanol partial oxidation, CuZnAl mixed oxide catalysts, layered double hydroxides

1. Introduction

Hydrogen is forecast to become a major source of energy in the future [1]. It is a clean burning and highly reactive fuel that offers high thermal efficiencies of 35–45% in comparison with 25–30% typical of normal petroleum fueled engines. Hydrogen-powered vehicles using fuel cells (e.g., polymer electrolyte fuel cell (PEFC)) are, therefore, under development in an effort to reduce CO_2 emissions that accelerate global warming [2]. In addition, fuel-cell-powered vehicles have virtually no emissions of particulates, NO_x, SO_x, etc. The paramount issue that is facing fuel cells right now is how to get the hydrogen fuel to the vehicle [3]. One solution to this problem is the on-board hydrogen generation from a suitable high energy density liquid fuel. Among various liquid fuels, methanol is considered to be a potential resource from which hydrogen can be extracted in three different processes: (i) methanol decomposition; (ii) steam reforming of methanol (SRM) and (iii) partial oxidation of methanol (POM; equations (1)–(3), respectively) [4–6]:

$$CH_3OH \rightleftharpoons 2H_2 + CO \quad \Delta H = 92.0\ \mathrm{kJ\,mol^{-1}} \tag{1}$$

$$CH_3OH + H_2O \rightleftharpoons 3H_2 + CO_2 \quad \Delta H = 49.4\ \mathrm{kJ\,mol^{-1}} \tag{2}$$

$$CH_3OH + (1/2)O_2 \rightleftharpoons 2H_2 + CO_2 \quad \Delta H = -192.2\ \mathrm{kJ\,mol^{-1}} \tag{3}$$

So far, the SRM reaction (equation (2)) was the only process considered for hydrogen production for fuel cell applications [5,7,8]. Unfortunately, the reaction produces a considerable amount of CO (>100 ppm) as a by-product. As for the application of PEFC, even traces of CO (>20 ppm) in the reformed gas deteriorate a Pt electrode and the cell performance is lowered dramatically [9]. A second-stage catalytic reactor has been suggested to remove the CO by water–gas shift reaction (WGSR) or CO oxidation [10] which, in turn, requires additional space and equipment cost.

An alternative method to produce hydrogen with lower amount of CO is by the POM reaction (equation (2)). When used in engines and vehicle technologies, the POM reaction offers some advantages compared to the SRM reaction as it requires air instead of steam and, it is an exothermic reaction, which does not require an external heat supply. Alejo et al. [6] have recently reported CuZn-based catalysts for the POM reaction. However, these catalysts deactivated during on-stream experiments. Addition of Al improved the catalyst stability but the methanol conversion rate reduced considerably. To avoid this inconvenience, we have employed CuZnAl ternary oxides obtained from thermal decomposition of CuZnAl hydroxycarbonates containing hydrotalcite as a major phase, since it is known that the nature of precursor and the method of preparation play an important role in the catalytic performance of CuZn-based methanol synthesis catalysts [11,12]. CuZnAl mixed oxides derived from hydrotalcite precursors have already been demonstrated to be efficient catalysts for the synthesis of methanol at low pressure [13].

* To whom correspondence should be addressed.

The objective of the present investigation is to develop an efficient catalytic system based on CuZnAl ternary oxides derived from corresponding hydrotalcite-like layered double hydroxides for the selective production of hydrogen for fuel cell applications by partial oxidation of methanol. We report our preliminary results in this communication.

2. Experimental

2.1. Catalyst preparation

CuZnAl-hydrotalcite-like hydroxycarbonate precursors with different Cu : Zn : Al atomic ratio were synthesized by a coprecipitation method at room temperature by reacting aqueous solutions containing a mixture of $Cu(NO_3)_2$, $Zn(NO_3)_2$ and $Al(NO_3)_3$ salts (depending upon the Cu : Zn : Al atomic ratio) and a mixture of NaOH (∼2 M solution) and Na_2CO_3 (∼0.3 M solution) at a constant pH (∼9) [14]. The (Cu + Zn)/Al atomic ratio in the starting solution was varied from 2 to 5. The resulting precipitate was aged at 65 °C for 30 min under stirring in a magnetic stirrer, filtered, washed with deionized water several times until the pH of the filtrate was 7 and then dried in an air oven at 70 °C overnight. The resulting powders were calcined in a furnace at 450 °C for 5 h and used as catalysts for the POM reaction.

2.2. Analytical techniques

The chemical compositions of the samples were determined by X-ray fluorescence (XRF) spectroscopy (Shimadzu Co. Lab center, XRF-1700 sequential X-ray fluorescence spectrometer). Powder X-ray diffraction (XRD) patterns of the samples were obtained using a Rigaku instrument (model RAD-1 VC) equipped with Ni-filtered Cu K_α radiation. Volume-weighted crystallite sizes of Cu were calculated using the Debye–Scherer equation, $t = 0.9\lambda/\beta\cos\theta$, where λ is the wavelength of the radiation (1.5418 Å), β is the line broadening of the peak due to the small crystallites (rad 2θ) and θ the corresponding angle of the diffraction peak. The full width at half maximum (FWHM) of the (111) reflection of copper was measured for the calculation of crystallite sizes [15]. A correction for instrumental broadening was also carried out: $\beta = (B^2 - b^2)^{0.5}$, where B is the total broadening and b is the instrumental broadening. The instrumental broadening was determined by the measurement of the FWHM of the (113) reflection of α-Al_2O_3 (corundum), and the estimated value of $b = 0.0021$ rad 2θ. The Cu surface areas of the catalysts were calculated from the crystallite sizes assuming a spherical particle model using the relation $t = 6/(SA\rho_{Cu})$, where ρ_{Cu} is the density of Cu (8.92 g cm^{-3}) [15].

The redox properties of the catalysts were investigated by the temperature-programmed reduction (TPR) method. About 50 mg of the calcined samples were placed in a quartz reactor (4 mm i.d.) and reduced in a stream of H_2 (5 vol% in Ar) at a heating rate of 5 °C min^{-1} up to 450 °C and dwelling at this temperature for 30 min. The hydrogen consumption due to the reduction of CuO phase was monitored continuously by a gas chromatograph (Shimadzu GC-8A) equipped with a thermal conductivity (TC) detector. Hydrogen consumption was calculated quantitatively from the TPR peak area, calibrated with standard CuO samples. The Cu surface areas, Cu dispersion and the Cu crystallite sizes were evaluated by the N_2O passivation method as described in the literature [16,17]. A normal TPR of the sample was performed first by heating the sample (heating rate 5 °C min^{-1}) from room temperature to 300 °C and keeping it at this temperature for 2 h (similar to the conditions employed in the POM reaction). The temperature was then reduced *in situ* to 60 °C and the catalyst was purged with He (flow rate 30 cm^3 min^{-1}) for about 15 min. N_2O passivation was performed by exposing the reduced catalyst to pure N_2O (Showa–Denko, >99.99% purity, flow rate 40 cm^3 min^{-1}) at 60 °C for about 1 h. After the N_2O passivation, the catalyst was purged with He (flow rate 30 cm^3 min^{-1}) to remove the residual oxidant and subsequently subjected to a second TPR to assess the amount of oxygen taken up by dissociative adsorption of N_2O. The TPR experiment was repeated as described above. The BET surface areas, pore volumes and pore size distributions of the calcined samples, before the reaction, were estimated by N_2 adsorption–desorption experiments at the liquid N_2 temperature using a Belsorp 28 SA (Japan), automatic gas adsorption apparatus.

2.3. Activity measurements

Catalytic experiments were performed in a packed-bed microreactor (4 mm i.d.) in the temperature range 200–245 °C at atmospheric pressure. The temperature of the catalyst bed was controlled (±0.2 °C) by a PID-SCR temperature controller (Ozawa Science). About 100 mg of the catalyst (particle size 0.25–0.30 mm) was sandwiched between quartz wool. The catalyst was first reduced *in situ* in a stream of H_2 (10 cm^3 min^{-1}) from room temperature to 300 °C with a temperature ramp of 5 °C min^{-1} and dwelling at this temperature for 2 h before cooling down to the reaction temperature. Liquid methanol at a rate of 1.5 or 2.0 cm^3 h^{-1} was fed into the pre-heater by means of a micro-feeder (model MF-2, Azumadenkikogyo Co. Ltd., Japan). Synthetic air (20.2 vol% of O_2 in N_2) at a rate of about 10–20 cm^3 min^{-1} and Ar (carrier gas, 40 cm^3 min^{-1}) were adjusted by means of a mass flow controller. The methanol concentration in the feed gas mixture was maintained well below 20 vol% in order to avoid any mass transfer effects. Because of a high exothermicity of the reaction, the catalyst bed temperature increased about 10 °C at the beginning of the reaction and, temperature equilibrium was established within 30 min. The reaction products were analyzed on-line using two gas chromatographs with

TC detectors: Shimadzu GC-8A and GC-320. The first GC (GC-8A) equipped with a 2 m long Porapak-Q column was able to detect the liquid products (water, methanol, formaldehyde, methyl formate and dimethyl ether), while the second GC (GC-320) equipped with a molecular sieve 13X was able to detect the gaseous products such as H_2, air, CO, CO_2 and CH_4. The catalytic activity was evaluated from the data collected between 5 and 7 h of on-stream operations. In order to check the stability of the catalyst, the reaction was also performed for a period of 24 h time-on-stream experiments at 200 °C. Blank runs conducted with an empty reactor in the temperature range 200–250 °C did not show any detectable methanol conversion.

3. Results and discussion

3.1. Characterization of the catalyst

The chemical compositions of the CuZnAl-LDH samples synthesized are presented in table 1. A Cu content of around 35 wt% has been maintained while varying the Zn and Al content in the sample. This is because earlier studies have demonstrated that a Cu–Zn catalyst containing 30–40 wt% of Cu is the most active for the POM reaction [6,7]. The XRD patterns of a few representative samples are shown in figure 1 (a)–(c), while the phases formed in each case are included in table 1 itself. Hydrotalcite (HT)-like layered double hydroxide (LDH; JCPDS file No. 38-487) is being observed as a major phase in all the samples [13]. The purity of the phase, however, depends on the (Cu + Zn)/Al atomic ratio. It can be noticed that a single phase corresponding to the LDH is obtained for the sample with a low (Cu + Zn)/Al ratio. As the Al content in the sample decreases, other phases such as aurichalcite, JCPDS file No. 7-743 and bayerite ($Al(OH)_3$; JCPDS file No. 20-11) are also formed besides the LDH phase. The sample CuZnAl-32LDH prepared by adding Na_2CO_3, without mixing NaOH, offered a new copper–zinc carbonate hydroxide (CZH; JCPDS file No. 38-154) as a main phase besides the LDH and malachite (JCPDS file No. 41-1390) phases. This is in contrast to the phases observed in an earlier study, in which a mixture of hydrozincite, malachite and auricalcite phases were formed by a similar coprecipitation method [6]. The results, therefore, reveal that both elemental composition and preparation parameters have a strong influence on the nature of phases formed in the Cu–Zn-based precursors.

Thermal decomposition of the CuZnAl-LDH precursors at 450 °C/5 h resulted in the formation of a mixture of poorly crystallized CuO and ZnO phases (figure 1 (d)–(f)). Other phases containing Cu/Zn/Al are most likely to be present, but because of their poor and highly disordered crystallization they could not be detected by XRD. The crystallinity of the calcined samples varies depending upon the elemental composition in their precursors. The BET surface areas and specific pore volumes increase with increasing (Cu + Zn)/Al atomic ratio. The calcined samples were also characterized by temperature-programmed reduction (TPR) experiments. Figure 2 shows the TPR profiles of CuZnAl-LDH samples calcined at 450 °C. All the samples exhibit a single reduction peak in the temperature range 200–300 °C. Calibration of the TCD signal with known amounts of CuO standard revealed that hydrogen consumption corresponds to the reduction of Cu^{2+} to Cu^0. Both, Al content and the preparation parameters have a strong influence in the reducibility of copper. The reduction peak is shifted toward low temperatures with decreasing Al content in the samples. On the other hand, the reduction peak of CuZnAl-32LDHcal is higher by about 40 °C compared to the CuZnAl-3LDHcal despite their similar chemical compositions (see table 1). This could be due to the formation of the CZH phase in preference to the LDH phase, as a result of a change in the preparation parameter.

TPR experiments were also performed for the determination of Cu surface areas and particle sizes of the catalysts by the N_2O passivation method [16,17]. For the sake of a better interpretation, we used exactly the same reduction conditions as employed in the POM reactions. The method is based on the measurement of the hydrogen consumption after complete oxidation of the catalyst, X, and after surface oxidation of the same catalyst, Y. After complete oxidation, X measures the total amount of reducible copper

Table 1
Chemical compositions and XRD phases of CuZnAl-LDH samples.[a]

Compound	Metal composition[b] (wt%)			(Cu + Zn)/Al atomic ratio[b]	XRD phase obtained
	Cu	Zn	Al		
CuZnAl-2LDH	35.3	44.1	20.6	1.61	LDH
CuZnAl-3LDH	36.7	48.1	15.2	2.32	LDH + AH + AC
CuZnAl-4LDH	39.3	48.9	11.8	3.13	LDH + AH + AC
CuZnAl-42LDH	37.6	50.7	11.7	3.17	LDH + AH + AC
CuZnAl-32LDH[c]	37.2	48.5	14.3	2.49	CZH + LDH + MT

[a] LDH = layered double hydroxide, JCPDS file 38-487; AH = $Al(OH)_3$ (bayerite), JCPDS file 20-11; AC = aurichalcite ($(Zn,Cu)_5(CO_3)_2(OH)_6$), JCPDS file 7-743; CZH = copper–zinc carbonate hydroxide ($(Cu_{0.2}Zn_{0.8})_5(CO_3)_2(OH)_6$), JCPDS file 38-154; MT = malachite ($Cu_2(CO_3)(OH)_2$), JCPDS file 41-1390.
[b] Chemical analysis results from XRF spectroscopy.
[c] Na_2CO_3 alone was used as a precipitating agent.

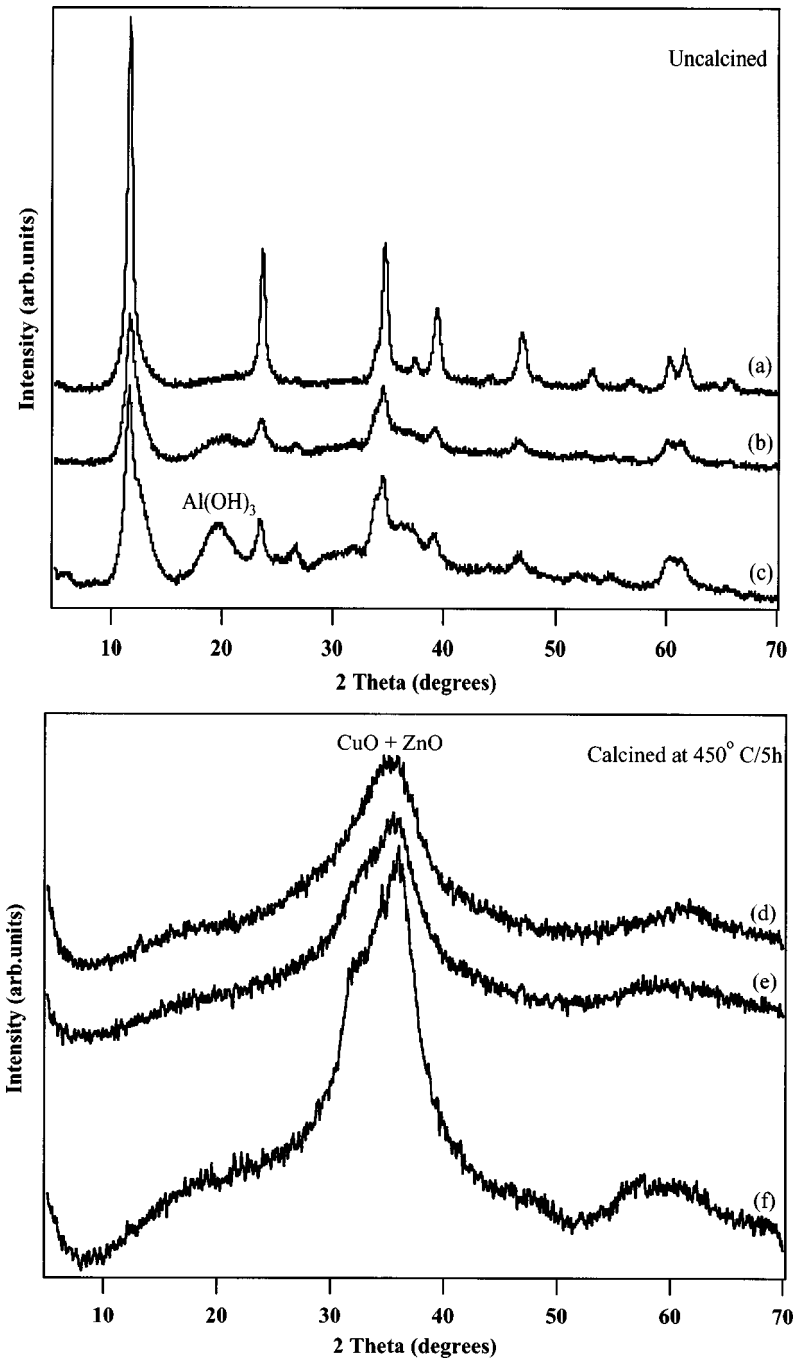

Figure 1. XRD patterns of (a) CuZnAl-2LDH, (b) CuZnAl-4LDH, (c) CuZnAl-42LDH, (d) CuZnAl-2LDHcal, (e) CuZnAl-4LDHcal and (f) CuZnAl-42LDHcal.

in the catalyst (equation (4)), whereas Y is a measure of number of surface Cu atoms (equation (5)):

for the total number of copper atoms,

$$\mathrm{CuO} + \mathrm{H_2} \rightarrow \mathrm{Cu} + \mathrm{H_2O}$$
$$\text{hydrogen consumption} = X; \qquad (4)$$

for the surface copper atoms,

$$\mathrm{Cu_2O} + \mathrm{H_2} \rightarrow 2\mathrm{Cu} + \mathrm{H_2O}$$
$$\text{hydrogen consumption} = Y. \qquad (5)$$

From the values of X and Y, the Cu surface area and particle sizes are calculated using relations (i) and (ii), respectively [15]:

$$\text{copper surface area (SA)} = \frac{2YN_{\mathrm{av}}}{XM_{\mathrm{Cu}}1.40 \times 10^{19}} \approx \frac{1353Y}{X}\ (\mathrm{m^2\,g^{-1}}), \qquad (\mathrm{i})$$

$$\text{copper particle size } (t) = \frac{6}{\mathrm{SA}\rho_{\mathrm{Cu}}} \approx \frac{0.5X}{Y}\ (\mathrm{nm}), \qquad (\mathrm{ii})$$

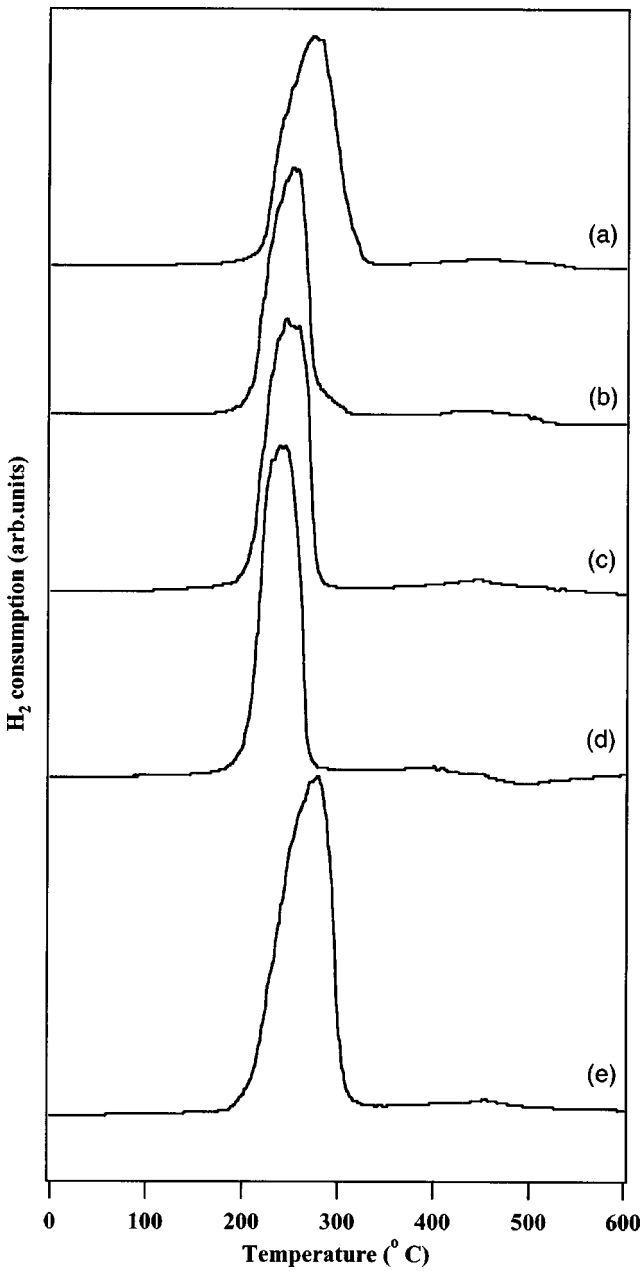

Figure 2. TPR profiles of (a) CuZnAl-2LDHcal, (b) CuZnAl-3LDHcal, (c) CuZnAl-4LDHcal, (d) CuZnAl-42LDHcal and (e) CuZnAl-32LDHcal.

where $N_{av} = 6.023 \times 10^{23}$ atoms mol^{-1}, M_{Cu} = relative atomic mass = 63.546 g mol^{-1} and ρ_{Cu} = density = 8.92 g cm^{-3}. The dispersion (D) of the Cu atoms is also calculated from the hydrogen consumption using relation (iii):

$$D = \frac{2Y}{X} \times 100\%. \qquad \text{(iii)}$$

The TPR profiles of completely oxidized samples (the first TPR corresponding to equation (4)) are similar to those shown in figure 2. The maximum rate of hydrogen consumption was observed around 250 °C, while the same was recorded around 150 °C in the second TPR (corresponding to equation (5)) after the N_2O passivation experiments. The Cu surface areas and particle sizes calculated from TPR and XRD are summarized in table 2. It is interesting to note that the values of Cu surface areas determined by TPR and XRD are comparable in most of the samples and they are in agreement with those determined by the similar TPR N_2O passivation method for Cu supported on various oxide supports [16].

3.2. Catalytic activity

Partial oxidation of methanol with air over CuZnAl-2LDHcal in a wide temperature range and different flow rates of argon and air revealed that the catalyst is active at a temperature as low as 200 °C. Analysis of the effluent gas indicated the presence of H_2 and CO_2 as major components with minor amount of CO. Other products such as formaldehyde, formic acid, methyl formate and dimethyl ether which are often formed by reactions of methanol over Cu-based catalysts could not be detected under the reaction conditions employed [17]. However, the reaction in the absence of O_2 or air offered a mixture of formaldehyde, CO and H_2 together with traces of methyl formate. It is known that formaldehyde decomposes to CO and H_2 above 200 °C over CuZn-based catalysts. Thus, the main reactions in the proposed route may be represented by equations (6)–(8):

$$CH_3OH + (1/2)O_2 \rightleftharpoons CO + H_2 + H_2O \qquad (6)$$

$$CH_3OH \rightleftharpoons CO + 2H_2 \qquad (7)$$

$$CO + H_2O \rightleftharpoons CO_2 + H_2 \qquad (8)$$

Table 2
Physico-chemical properties of CuZnAl-LDH derived catalysts.

Catalyst	BET surface area ($m^2\,g^{-1}$)	Pore volume ($cm^3\,g^{-1}$)	H_2 consumption[a] (mmol g^{-1})	TPR-N_2O passivation method			XRD line broadening method[b]	
				Cu surface area ($m^2\,g^{-1}$)	Particle size (Å)	Cu dispersion (%)	Cu surface area ($m^2\,g^{-1}$)	Particle size (Å)
CuZnAl-2LDHcal	56	0.181	3.3	261	26	38.6	197	34
CuZnAl-3LDHcal	71	0.263	3.6	232	29	34.3	183	37
CuZnAl-4LDHcal	84	0.406	6.0	226	30	33.4	146	46
CuZnAl-42LDHcal	108	0.428	4.2	291	23	43.1	154	44
CuZnAl-32LDHcal	70	0.264	3.6	276	25	40.8	87	77

[a] Hydrogen consumption in the first TPR of N_2O passivation experiments.
[b] Catalysts (100 mg) reduced in H_2 stream at 300 °C/2 h in the catalytic reactor.

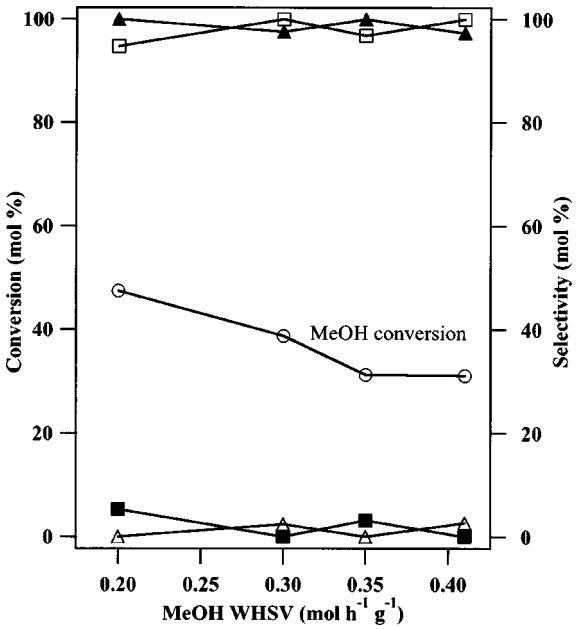

Figure 3. Effect of methanol space velocity on catalytic performance over CuZnAl-2LDHcal: (□) H_2 selectivity, (■) H_2O selectivity, (▲) CO_2 selectivity and (△) CO selectivity; $O_2/CH_3OH = 0.25$.

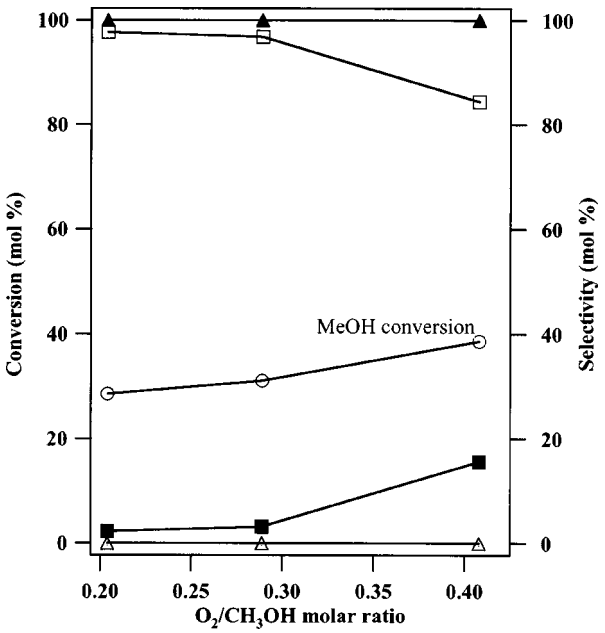

Figure 4. Effect of O_2/CH_3OH molar ratio on the catalytic performance over CuZnAl-2LDHcal: (□) H_2 selectivity, (■) H_2O selectivity, (▲) CO_2 selectivity and (△) CO selectivity; WHSV = 0.30 mol h^{-1} g^{-1}.

The reaction over unreduced catalysts offered a mixture of CO_2 and H_2O as the main products because of a complete combustion of methanol. A systematic study was then undertaken after reducing the catalyst in a stream of H_2 at 300 °C (cf. TPR results) to optimize the reaction operating conditions.

3.2.1. Effect of methanol space velocity

Figure 3 shows the effect of methanol space velocity (WHSV) on the catalytic performance over CuZnAl-2LDHcal. The methanol conversion decreases with increasing space velocity until 0.35 mol h^{-1} g^{-1} and then remains unchanged. On the other hand, the methanol space velocity does not influence the product selectivity much. It can be seen that the selectivity of H_2 and CO_2 remains around 100% throughout the experiment. In the present study, a methanol space velocity between 0.30 and 0.35 mol h^{-1} g^{-1} has been chosen for the evaluation of the performance of the catalysts in the POM reaction.

3.2.2. Effect of O_2/CH_3OH molar ratio

Preliminary studies using O_2 as an oxidant with an O_2/CH_3OH molar ratio of 0.5 (the stoichiometric amount required) offered a mixture of H_2, CO_2, H_2O and CO probably because of combustion of methanol over these catalysts. Hence, we used air (20.2 vol% of O_2 in N_2 gas) instead of O_2. Figure 4 shows the effect of O_2/CH_3OH molar ratio on the catalytic performance over CuZnAl-2LDHcal at 200 °C. It can be observed that the methanol conversion increases from about 27 to 40% upon doubling the O_2/CH_3OH ratio (from 0.2 to 0.4). The formation of CO is not detected and the selectivity of CO_2 remains 100% throughout the study. On the other hand, the H_2 selectivity decreases with consequent increase in the selectivity of H_2O. This could be due to the fast oxidation of H_2 produced in the reaction [18]:

$$H_2 + (1/2)O_2 \rightleftharpoons H_2O \quad (9)$$

Furthermore, since the O_2/CH_3OH molar ratio used in the present study is less than the stoichiometric amount required (0.5), the steam reforming reaction (equation (2)) can be expected between H_2O formed in the reaction (equation (6)) and excess of methanol to produce H_2 and CO_2.

3.2.3. Effect of temperature

The effect of temperature on catalytic performance of a series of CuZnAl-LDH derived catalysts is depicted in figure 5. The methanol conversion increases with increasing reaction temperature. However, the increase is less pronounced in the case of CuZnAl-42LDHcal and the conversion decreases above 230 °C. On the other hand, a conversion of about 80% could be achieved at 245 °C over CuZnAl-4LDHcal. The catalytic activity at 200 °C seems to depend on the (Cu + Zn)/Al atomic ratio. The observed activity trend could be best correlated with the Cu surface area and the Cu metal dispersion which, intern, depends on the (Cu + Zn)/Al atomic ratio. It is clear from the data provided in table 2 that the Cu surface area and Cu dispersion determined by the N_2O passivation method decrease with increasing the (Cu + Zn)/Al ratio. Hence, the catalytic activity at 200 °C also decreases in the same order. However, CuZnAl-42LDHcal displayed the highest Cu surface area of 291 m^2 g^{-1} and highest Cu dispersion of 43.1% and, as a consequence, exhibited the highest catalytic activity. These results reveal that the Cu exposed on the surface is essential for an active catalyst. A re-

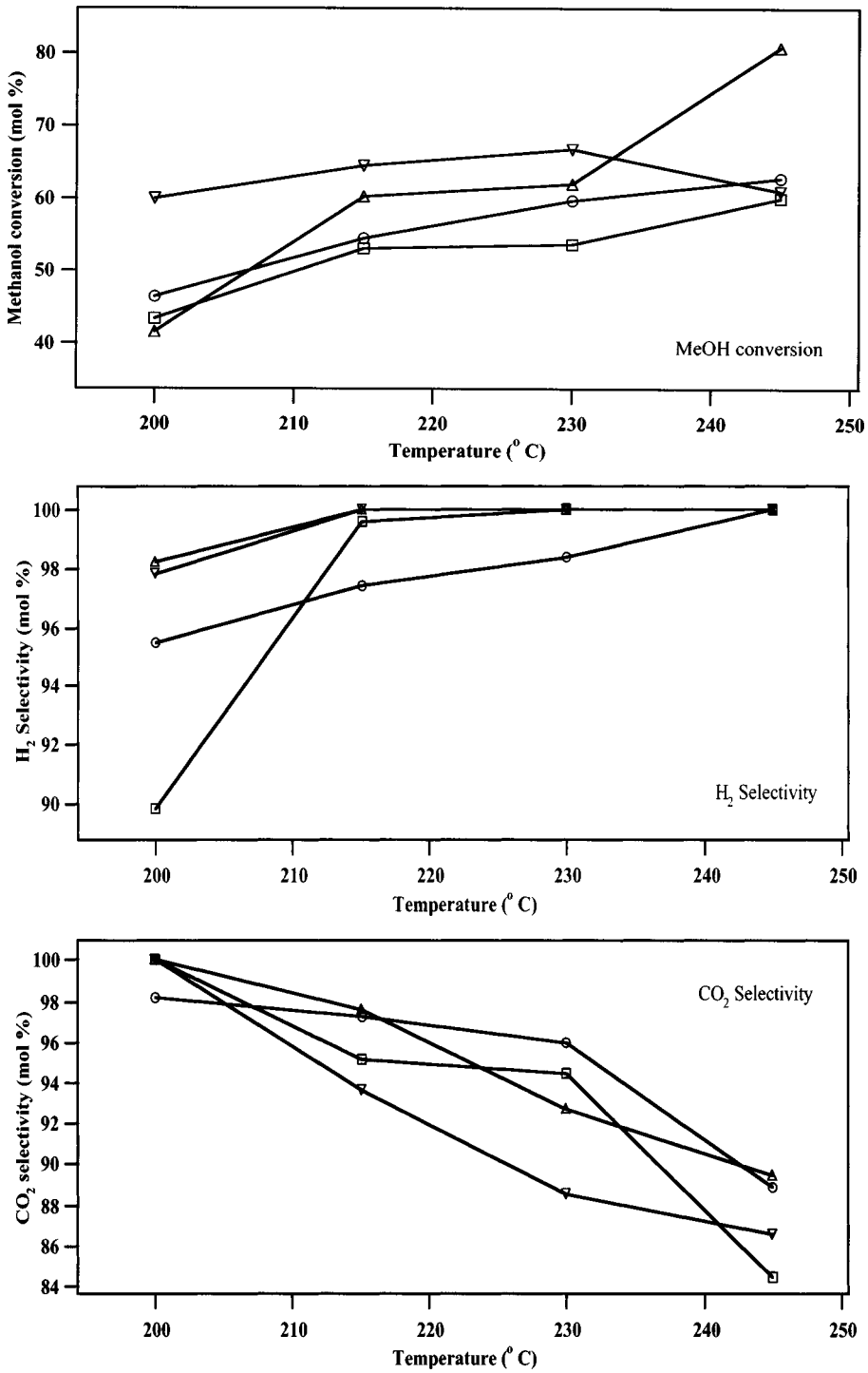

Figure 5. Effect of temperature on catalytic performance over various CuZnAl-LDHcal catalysts: (○) CuZnAl-2LDHcal, (□) CuZnAl-3LDHcal, (△) CuZnAl-4LDHcal and (▽) CuZnAl-42LDHcal; WHSV = 0.30 mol h^{-1} g^{-1}; O_2/CH_3OH = 0.29.

cent spectroscopic study [19] using ESR and XPS on the CuZnAl mixed oxide catalysts reported that catalysts with higher Cu dispersion would exhibit Cu–Al interactions at their surfaces in the calcined states of the samples. The presence of Al would contribute to a significant extent to the dispersion of entities of oxidized Cu at the surface of the calcined samples, both by the formation of specific surface phases between Cu and Al and by the stabilization of isolated Cu^{2+} species. Upon subsequent reduction, these dispersed cations might behave as anchoring points for the formation of Cu particles, leading to higher Cu surface areas and, consequently, to the higher catalytic activity.

The product selectivity also depends on the reaction temperature. The H_2 selectivity increases at the expense of H_2O with increasing reaction temperature. Both CuZnAl-

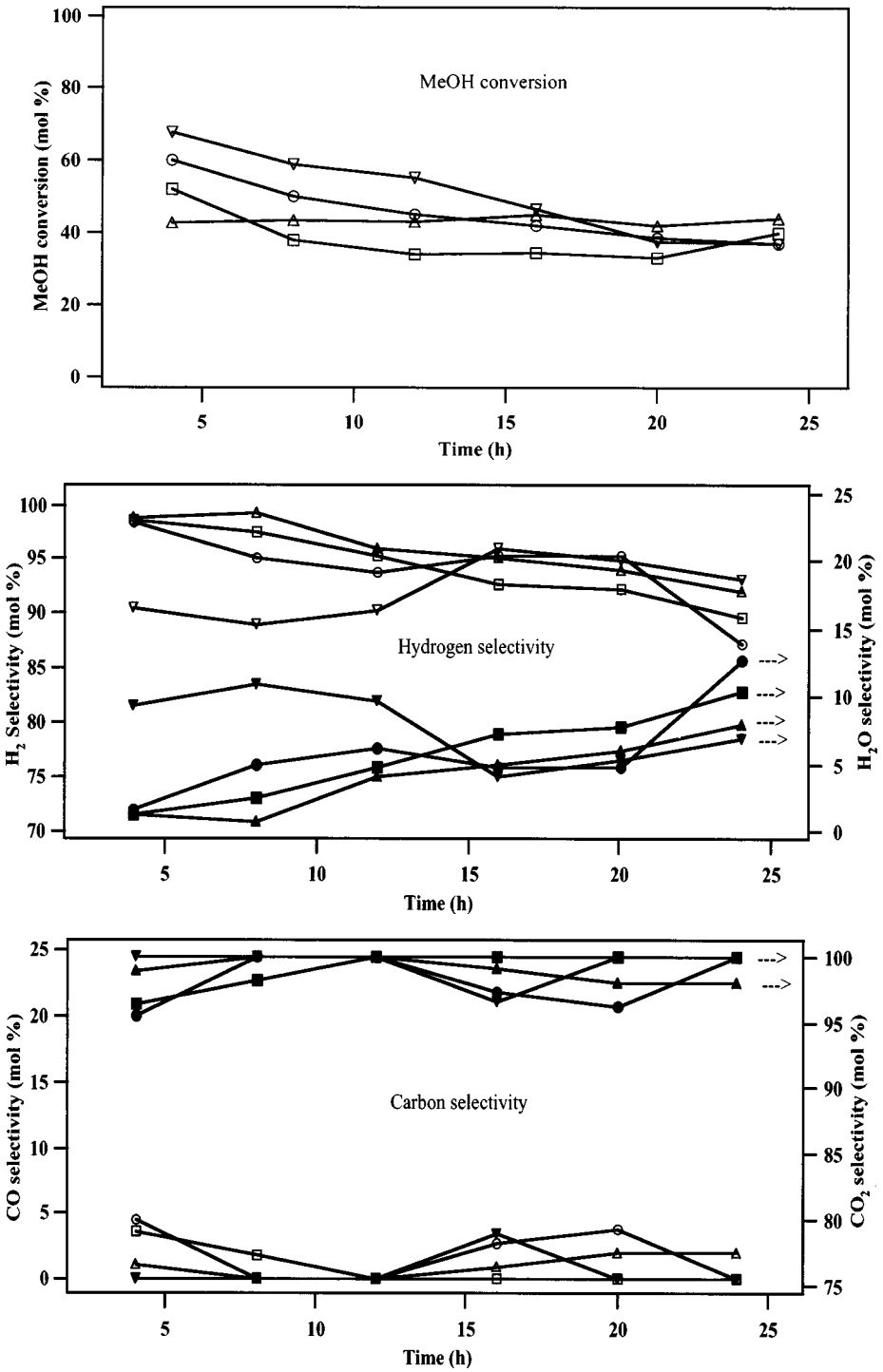

Figure 6. Time-on-stream experiments over various CuZnAl-LDHcal catalysts: (○) CuZnAl-2LDHcal, (□) CuZnAl-3LDHcal, (△) CuZnAl-4LDHcal and (▽) CuZnAl-42LDHcal; MeOH WHSV = 0.35 mol h^{-1} g^{-1}; O_2/CH_3OH = 0.29.

4LDHcal and CuZnAl-42LDHcal exhibited a higher selectivity of H_2 (>98%) even at 200 °C. On the other hand, the CO_2 selectivity decreases markedly with increasing reaction temperature. The CO is virtually not produced at 200 °C and its production rate increases steeply at the expense of CO_2 upon increasing the reaction temperature. The decrease in selectivity of both H_2O (increase in selectivity of H_2) and CO_2 and concomitant increase in the CO selectivity with increasing temperature suggests that CO is produced by a reverse water–gas shift reaction (equation (8)) at higher temperatures. A maximum CO concentration of about 500 ppm has been recorded up to about 50% methanol conversion. Although this CO concentration is above the tolerable limit of the PEFC (<50 ppm), this amount is considerably less than that produced in the steam reforming reaction [10].

The nature of phases formed in the precursor of the catalyst plays an important role in the product selectivity. For instance, the catalyst (CuZnAl32-LDHcal), derived from CuZnAl-32LDH containing the CZH as a major phase, produced considerable amount of dimethyl ether besides H_2 and CO_2 under the same reaction conditions. Similar results are also observed over the catalyst derived from CuZnAl-5LDH because of the co-formation of the CZH phase together with the LDH phase. From these observations it can be inferred that the CuZnAl catalysts derived from LDH as a major phase are more selective for the hydrogen production by the POM reaction.

3.2.4. Stability of the catalyst

In order to investigate the stability of the catalysts during the POM reaction, time-on-stream experiments were performed at 200 °C over all the catalysts for a period of 24 h and the results are displayed in figure 6. It can be seen that, except CuZnAl-4LDHcal, there is a small initial deactivation over other catalysts. However, this deactivation seems to be less significant as in many cases the rate of methanol conversion regains the initial value after few hours of continuous operation. On the other hand, the methanol conversion remained almost unchanged throughout the period in the case of CuZnAl-4LDHcal. As far as the product selectivity is concerned, there is a minor drop in the selectivity of H_2 at the expense of H_2O. This is probably due to the oxidation of H_2 with O_2 (equation (9)) or due to the oxidation of surface Cu atoms into Cu^+/Cu^{2+} under the reaction conditions employed. However, it is interesting to note that the selectivity of CO and CO_2 remains almost unaffected during the 24 h of on-stream operation. Only traces of CO (<50 ppm) are produced over at least a few catalysts (CuZnAl-4LDHcal and CuZnAl-42LDHcal) at 200 °C under the present experimental conditions.

4. Conclusions

CuZnAl ternary oxide catalysts derived from hydroxycarbonate precursors containing hydrotalcite-like layered double hydroxide display great activity for methanol conversion and high selectivity for H_2 and CO_2. The catalytic activity decreases with increasing (Cu + Zn)/Al atomic ratio in the precursors because of a decrease in the Cu metal surface areas and Cu metal dispersion and increase in the Cu particle sizes. At 200 °C, a methanol conversion of 40–60% could be attained over these catalysts with high selectivity (>90%) of H_2 and (>95%) CO_2. The undesirable by-product, CO, was not produced at a methanol space velocity of 0.30 mol h^{-1} g^{-1} and O_2/CH_3OH molar ratio of 0.29 at this temperature. The existence of Cu–Al interactions at the surfaces in the calcined state of the catalysts is assumed to be responsible for the higher catalytic performance. The catalyst deactivation during 24 h of continuous operation is insignificant over these catalysts. Increase in reaction temperature increases the methanol conversion and H_2 selectivity with decrease in selectivity of CO_2 at the expense of CO. The total CO concentration in the outflow gas stream is relatively less compared to the amount produced in the steam reforming reaction over similar Cu-based catalysts. A combined partial oxidation–steam reforming of methanol over these catalysts is currently in progress to produce CO-free H_2 fuel and the results will be reported in the near future.

Acknowledgement

We thank Dr. F. Ohashi for XRF spectroscopy for chemical analysis. One of the authors (SV) is grateful to the Japan International Science and Technology Center (JISTEC) for the award of a STA fellowship.

References

[1] J.N. Armor, Appl. Catal. A 176 (1999) 159.
[2] V.M. Schmidt, P. Brockerholf, B. Hohlein, R. Menzer and U. Stimming, J. Power Sources 49 (1994) 299.
[3] K.S. Betts, Environ. Sci. Tech./News (1 March 1999) 107A.
[4] W.-H. Cheng and H.H. Kung, *Methanol Production and Use* (Dekker, New York, 1994) p. 1.
[5] H. Kobayashi, N. Takezawa and C. Minochi, J. Catal. 69 (1981) 487.
[6] L. Alejo, R. Lago, M.A. Pena and J.L.G. Fierro, Appl. Catal. A 162 (1997) 281.
[7] T. Huang and S. Wang, Appl. Catal. 24 (1986) 287.
[8] B.A. Peppley, J.C. Amphlett, L.M. Kearns and R.F. Mann, Appl. Catal. A 179 (1999) 21.
[9] H.-F. Oetjen, V.M. Schmidt, U. Stimming and F. Trila, J. Electrochem. Soc. 143 (1996) 3838.
[10] K. Sekizawa, S. Yano, K. Eguchi and H. Arai, Appl. Catal. A 169 (1998) 291.
[11] T. Fujitani and J. Nakamura, Catal. Lett. 56 (1998) 119.
[12] G.E. Parries and K. Klier, J. Catal. 97 (1986) 374.
[13] C. Busetto, G. Del Piero, G. Mamara, F. Trifirò and A. Vaccari, J. Catal. 85 (1984) 260.
[14] S. Velu, K. Suzuki, M. Okazaki, T. Osaki, S. Tomura and F. Ohashi, Chem. Mater. 11 (1999) 2163.
[15] C.J.G. Grift, A.F.H. Wielers, B.P.J. Joghi, J. van Beijnum, M. de Boer, M. Versluijs-Helder and J.W. Geus, J. Catal. 131 (1991) 178.
[16] G.C. Bond and S.N. Namijo, J. Catal. 118 (1989) 507.
[17] I.E. Wachs and R.J. Madix, J. Catal. 53 (1978) 208.
[18] M.L. Cubeiro and J.L.G. Fierro, J. Catal. 179 (1998) 150.
[19] R.T. Figueiredo, A. Martinez-Arias, M.L. Granados and J.L.G. Fierro, J. Catal. 178 (1998) 146.
[20] W. Cheng, Appl. Catal. A 130 (1995) 13.